Indentation-induced deformation localisation in Zr–Cu-based metallic glass

Indentation-induced deformation localisation in Zr-Cu-based metallic glass

V. Nekouie[a], G. Abeygunawardane-arachchige[a], U. Kühn[b], A. Roy[a] and V. V. Silberschmidt[a]

[a] Wolfson School of Mechanical and Manufacturing Engineering, Loughborough University, Leicestershire, UK
[b] IFW Dresden, Institute for Complex Materials, Helmholtzstraße 20, D-01069, Dresden, Germany

*Corresponding author's e-mail: A.Roy3@lboro.ac.uk
Tell: +441509227637; fax: +441509227502

Add: Wolfson School of Mechanical and Manufacturing Engineering, Loughborough University, UK

Abstract. It has been well documented that the plastic deformation of bulk metallic glasses is localised in thin shear bands. In order to comprehensively understand deformation mechanisms of BMGs, it is necessary to investigate formation of shear bands and related deformation. Nano-indentation studies with a spherical indenter were carried out to characterise shear-band localisation on a surface of Zr-Cu-based metallic glass. The load-displacement diagram of an indentation cycle reflects an elastic deformation followed by the first pop-in at around 4 mN. In addition, an alternative technique is proposed to characterise a plasticity mechanism through the evolution of localised shear bands beneath the indentation – wedge indentation. It is found that a hemicylindrical region of shear bands is formed beneath the indentation zone in this case.

Key words: Metallic glass, Indentation, Shear-band localisation, Finite-element analysis.

1. Introduction

Modern high-tech industries rely heavily on manufacture and synthesis of advanced materials that are stronger than traditional ones and at the same time environmentally sustainable. Demands in the areas of microelectronics, MEMS (micro-electromechanical systems), miniaturised biomedical devices and implants as well as micro-robotics typically require component sizes at micro- to meso-length scale where ruggedness, shock resistance, bio-compatibility and

DOI: 10.1016/j.jallcom.2013.12.002 To appear in: Journal of Alloys and Compounds, 2013

environmental sustainability are of paramount importance. Bulk metallic glasses (BMGs) are an emerging class of engineering materials with many desirable and unique properties, which are ideally suited for these applications. In the last few decades research has led to the discovery and development of new BMGs in a variety of multi-component alloy systems including the rare-earth-based ones that vitrify with a remarkable ease during conventional solidification making thicknesses of several centimetres and weighing several kilograms [1]. BMGs have received much scientific and technological attention due to their unique combination of physical, chemical and mechanical properties such as high ratio of elastic limit to Young`s modulus, higher fracture toughness (when compared to crystalline counterparts of the same composition) [2,3]. Typically, inorganic glasses are brittle at room temperature, exhibiting a smooth fracture surface as a result of mode-I brittle fracture. BMGs, to the contrary, generally deform by localised shear deformation at room temperature and show enhanced small-scale ductility. These characteristics of plasticity impart distinct features to the mechanical behaviour of BMGs such as flow softening, pressure sensitivity and ductile-to-brittle transition [4]. An excellent review of deformation mechanisms in BMGs in presented in Greer et al. [10]. Thus, studying the influence of plasticity at microscopic length scales becomes essential for the development of robust modelling frameworks for BMGs

In this study, a Zr-Cu-based BMG is characterised across several length scales. A numerical model is developed to study localisation of plastic deformation in BMGs.

2. Experimental procedure

A Zr-Cu-based alloy with a nominal composition of $Zr_{48}Cu_{36}Al_8Ag_8$ (at%) was critically evaluated. The alloy was initially produced by arc-melting on a water-cooled copper mold under a high purity argon atmosphere at IFW Dresden, Institute for Complex Materials, Germany. The ingot was re-melted at least three times to obtain homogeneity. Furthermore, from this alloy ingot rectangular beam-shaped samples with a cross-section of 10 mm × 2 mm and a nominal length of 80 mm were prepared by suction casting into a copper mould.

Three different experimental tests were employed to characterise the mechanical behaviour of the BMG samples. First, macroscopic three-point bending tests were carried out. For these tests, the supplied beam samples were cut into specimens with the length of 40 mm. The bending tests were conducted with an Instron 3345 testing machine. A biaxial strain gauge was attached to the specimen to measure strains in the axial and transverse directions during the loading process. The load was applied with the displacement rate of 2 mm/min. Additionally, high-precision dynamical mechanical relaxation measurements were performed with a

DOI: 10.1016/j.jallcom.2013.12.002 To appear in: Journal of Alloys and Compounds, 2013

DMA system (Mettler Toledo-SD TA861). The experimental frequency range was from 0.2 Hz and 160 Hz at constant temperature. Experiments were repeated several times to obtain sufficient statistically significant test data.

Next, indentation tests were conducted with a Nano Test system (Micro Materials Ltd.) equipped with a spherical indenter, made of diamond, with a radius of 5 μm. The specimens for this study were cut from the supplied beam samples and polished to mirror-like finish with average roughness of around 5 nm. All the tests were conducted in a displacement-control mode, with multiple unloading-reloading cycles performed. The loading and unloading rates were 0.1 mN/s and 2 mN/s for the incremental loading-unloading experiments, followed by the holding time of 1 s for all experiments. The maximum applied indentation displacement ranged from 20 nm to 2000 nm.

Finally, a wedge-indentation experiment was developed. This was carried out to (1) observe the evolution of shear bands in BMG specimens and (2) allow for simplified analytical and numerical modelling schemes. A wedge indenter made of titanium, with an angle of 60° and an edge radius of 43 μm, height of 26 μm and width of 42 μm, was designed and manufactured in-house. A Taylor Hobson precision `Talysurf CLI 2000` system was used to measure the radius and height of the edge (Fig. 1(b)). Appropriate fixtures were designed to attach the indenter to the Instron 3345 testing machine (Fig. 1). Testing was carried out on the beam-shaped samples in a compression mode with a constant displacement rate 0.05 mm/min. Maximum loads applied varied from 2 kN to 4 kN for wedge indentation. The length of the wedge indenter was much larger than the specimen's width, resulting in nearly 2D loading regime.

3. Experimental results and discussion

The macroscale tests in bending consistently gave an elastic modulus (E) of 86 GPa with a Poisson's ratio of 0.35. The accuracy of frequency-dependent modulus measured with DMA was better than 2%. The obtained elastic modulus was observed to be less than what is typically reported in literature ~110 GPa. The latter magnitude was measured with ultrasonic techniques; this may be the reason for the discrepancy between the magnitudes. Simplicity of the bending test in determining elastic moduli is worth considering in comparison to tensile tests, which often suffer from fixation, gripping and alignment problems. The DMA studies effectively confirm the validity of the obtained results.

To characterise the initiation of the first plastic event, loading-unloading studies were conducted in nano-indentation, with the incrementally increased load. In Fig. 2, loading-unloading diagrams are presented for an imposed peak load of 3 mN and 7 mN. In a former case, no appreciable plasticity was observed (represented by AB in Fig. 2), and the deformation was assumed to be purely

elastic. However, in a latter loading case, a significant plastic event was observed at ~4 mN, which is considered to be the first 'pop-in' event (represented by CD in Fig. 2). This value is rather close to that obtained in tests of a Zr-Cu-Al alloy studied elsewhere [5]. In our experiments another pop-in event was found to occur at a load of 5.5 mN. The presented load-displacement plot is a typical example of several tests, which showed closely correlated first pop-in events. Unfortunately, due to the nature of the experiment conducted, there is no possibility of observing the nucleation and initial propagation of shear bands, as it occurs inside the material volume. A bonded-interface technique [6], which was used to reveal the deformation morphology under indenters, has an inherent problem with traction-free surfaces that are naturally created when the specimen is split.

In order to assess the evolution of shear bands in the BMG material, loading-unloading cycles were carried out at higher load magnitudes with the aim of observing shear steps on the material's surface. Such steps in spherical indentation of BMG were found at loads in excess of 100 mN (Fig. 3). Incidentally, the elastic modulus obtained from the unloading part of the load-displacement curves indicates that $E = 86$ GPa in other tests is accurate.

The primary motivation in performing wedge indentation studies was to characterise the initiation of shear bands in the material and correlate this to the first 'pop-in' event in indentation. Wedge indentation tests were conducted at high incrementally-changed peak loads (1 kN to 4 kN in increments of 0.5 kN). The choice of Ti as an indenter material was linked to it's Young's modulus in excess of 100 GPa (hence, stiffer than the tested BMG material). Additionally, the indenter was checked for permanent deformation at the end of each experiment and no measurable geometry change was observed. Thus, it may be assumed that the indenter suffered only elastic deformation during the experiment. At loads in excess of 4 kN, plastic deformation was observed to occur in the wedge. Figure 4 shows the evolution of shear bands on the front surface of the indented beam with increasing loads. It is to be noted that each experiment was performed at a distinct surface location with a minimum distance of 1 mm between each indents. At loads in excess of 1.5 kN, shear bands were observed to appear in the material. Due to the nature of the test, it is fair to assume that the shear bands extend through the entire material volume in the transverse direction. The shear bands formed a distinct circular pattern on the surface with almost equidistant bands with increasing loads. Based on the above observations, it is reasonable to deduce that a section of a cylindrical surface of shear bands was formed beneath the indenter. The shear bands localise near the tip once the initial shear bands are formed; this can be seen in Fig. 4(b) when compared to Fig. 4(a). The additional shear bands localise near the indenter tip.

DOI: 10.1016/j.jallcom.2013.12.002 To appear in: Journal of Alloys and Compounds, 2013

This indicates that once a shear band is formed (at loads in excess of 1.5 kN and at or below 2 kN) the deformation concentrates in the region formed by the free surface and the slipped region at higher loads; as a result, further localisation happens within this domain. The validity of the hypothesis may be checked by sectioning the component to assess the nature of the shear bands across the beam width; however, there are some practical challenges in machining components that inevitably introduce secondary features due to the sectioning process.

4. Finite-element modelling studies

Based on the experimental studies carried out, a numerical model was developed representing the material response of the studied amorphous alloy. The general-purpose finite-element software, ABAQUS 6.12, was used to model a wedge-indentation experiment. Due to the nature of the experiment, a 2D plane strain assumption is adequate for our modelling needs. The wedge was modelled as an analytic rigid body reproducing geometry of the wedge, whereas the BMG material, with a domain of 2 mm × 2 mm was discretised using 4-node bilinear, reduced-integration (CPE4R) elements with hourglass control. A finer mesh was used to discretize the zone in proximity to the indenter in order to capture the stress variation accurately. Displacements at the bottom of the specimen were constrained, while the indenter moved into the workpiece sample via displacement imposed on the reference point of the indenter's surface. The Coulomb's friction law with a coefficient of friction $\mu = 0.03$ was used to model the contact interaction between the indenter and the surface of the BMG sample. The value was chosen after carrying out calibration tests. The mechanical behaviour of BMG was assumed to closely represent the constitutive description of a linear Drucker-Prager material model. The Drucker-Prager yield criterion (F) is represented as

$$F = t - p\tan(\beta) - d$$

where t, the pseudo-effective stress, is defined as

$$t = 0.5q\left[1 + \frac{1}{K}\right] - \left(1 - \frac{1}{K}\right)\left(\frac{r}{q}\right)^3.$$

Here, β is the friction angle of the material (the slope of the linear yield surface in the $p-t$ stress plane), p is hydrostatic pressure, d is the cohesion parameter, r is the third invariant of the deviatoric stress, K is the ratio of the yield stress in tri-axial tension to that in tri-axial compression and q is von Mises

DOI: 10.1016/j.jallcom.2013.12.002 To appear in: Journal of Alloys and Compounds, 2013

equivalent stress. For linear Drucker Prager model, the flow potential, g, is defined as

$$g = t - p\tan(\psi)$$

where, ψ is the dilation angle in the $p-t$ plane. The original Druger-Prager formulation is recovered by setting $\psi = \theta$ and $r = 1$. Table 1 lists all the relevant parameters used in the model. Some data on the post-yield response is available in [7].

The finite-element model developed is shown in Fig. 5(a),(b). The mesh size was sufficiently refined to account for the local stress variation. The element size in the vicinity of the wedge indenter was 3.77 μm × 3.77 μm. The contour plot of maximum shear stresses is shown in Fig. 5 (c) under an imposed load of 2 kN. As expected, a large plastic zone was formed under the indenter tip commensurate with prior experiments [8,9]. Comparing the maximum shear stress distribution in the model to the shear-band distribution obtained at an applied load of 2 kN (Fig. 4(a)), a reasonable match between the spatial depth (marked in Fig. 5(c)) and the depth, at which the shear bands formed in the experiment (Fig. 4(a)), was observed. This indicates that the maximum-shear-stress criterion (of ~2 GPa) is suitable to describe the initiation of shear localisation in the material. The presented material model is somewhat limited, as there is no underlying mechanism to account for material separation once the maximum shear stress is obtained. Also there is no underlying mechanics to account for shear-band evolution. Thus, the next step of our research will be development of strain-gradient-based constitutive material models, accounting for nucleation and evolution of shear-bands in a physically sound way. This will allow for shear band localisation (at the wedge tip, as observed in Fig. 4(b)) once shear bands are nucleated.

5. Conclusions

In this study, indentation techniques were extensively used to first study the elastic deformation of a Zr-Cu-based BMG alloy, followed by a systematic analysis of initiation and evolution of shear-band localisation in the indented material. Our results obtained with the suggested wedge-indentation technique demonstrate the initiation of shear bands in the material volume. This technique is particularly useful for materials scientists for development of appropriate constitutive models that characterise plastic events in the amorphous material in the small-length scale. Some results of initial numerical simulations of deformation processes demonstrate that a maximum-shear-stress criterion can be used in developing constitutive models of BMG to characterise shear-band localisation in BMGs.

DOI: 10.1016/j.jallcom.2013.12.002 To appear in: Journal of Alloys and Compounds, 2013

6. References

[1] C.J. Byrne, M. Eldrup, Science. 321 (2008) 502-503.
[2] S. Vincent, J. Basu, B.S. Murty, J. Bhatt, Mater. Sci. Eng., A 550 (2012) 160-166
[3] A. R. Yavari, Nature. 439 (2006) 405-406.
[4] C.A. Schuh, T. Hufnagel, U. Ramamurty, Acta Mater 55 (2007) 4067-40109.
[5] C.E. Packard, C.A. Schuh, Acta Mater. 55 (2007) 5348-5358.
[6] V. Keryvin, X.D. Vu, V.H. Hoang, J. Shen, Compd. 5045(2010) 541-544.
[7] Q.Z. Zhang, W. Zhang, G.Q. Xie, A. Inoue, Int. J. Mater. Sci. 17 (2010) 208-213.
[8] B. Yang, L. Riester, T.G. Nieh, Scr. Mater. 54 (2006) 1277-1280.
[9] C.A. Schuh, T.G. Nieh, A survey of instrumented indentation studies on metallic glasses, J. Mater. Res. 19 (2004) 46-56.
[10] A.L. Greer, Y.Q. Cheng, E. Ma, Mater Sci Eng R. 74 (2013) 71-132

DOI: 10.1016/j.jallcom.2013.12.002 To appear in: Journal of Alloys and Compounds, 2013

FIGURE CAPTIONS:

Fig. 1. Two parts of assembled wedge indenter (a), its main dimensions (b) and Experimental setup for wedge indentation (c)

Fig. 2. Typical load-displacement response at loading rate of 0.1 mN/s showing cyclic loading to determine purely elastic deformation (AB) and first pop-in (CD)

Fig. 3. Indentation load-displacement curves of ZrCu-based BMG for incremental loading-unloading at loading rate of 2 mN/s. The insets show evolution of shear-band patterns with increasing load

Fig. 4. Evolution of shear band localisation with increasing loads: (a) 2 kN; (b) 2.5 kN and (c) 4 kN

Fig. 5. (a) Finite element model of wedge indentation, (b) expanded view of the indenter geometry and the mesh density of the material, (c) maximum shear stress contour plot of the material after indentation with a 2 kN load.

TABLE CAPTIONS:

Table. 1. Modelling parameters used in FEM simulation

DOI: 10.1016/j.jallcom.2013.12.002 To appear in: Journal of Alloys and Compounds, 2013

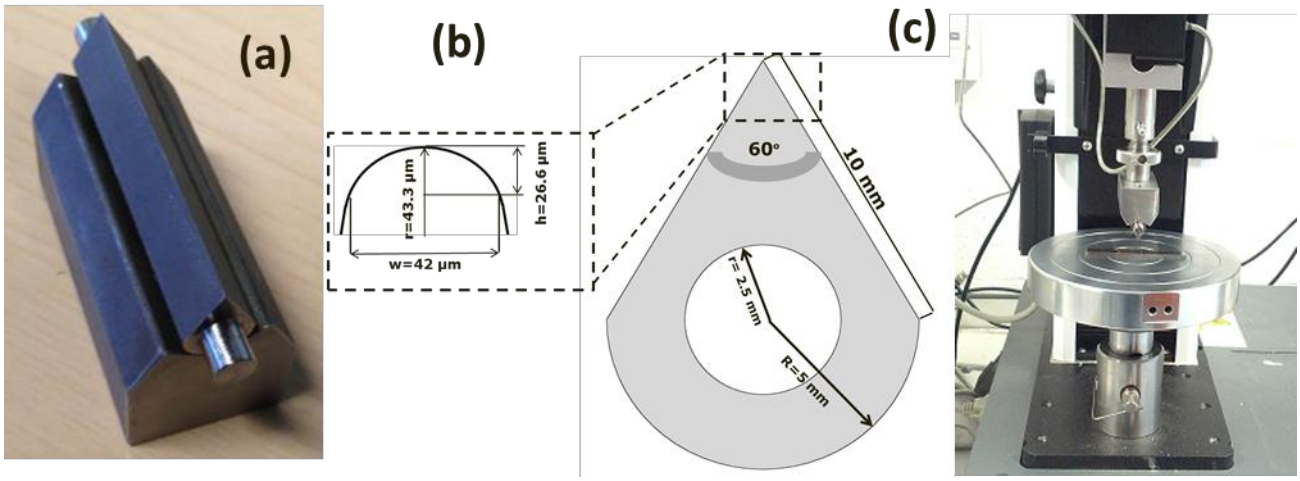

Fig. 1. Two parts of assembled wedge indenter (a), its main dimensions (b) and Experimental setup for wedge indentation (c)

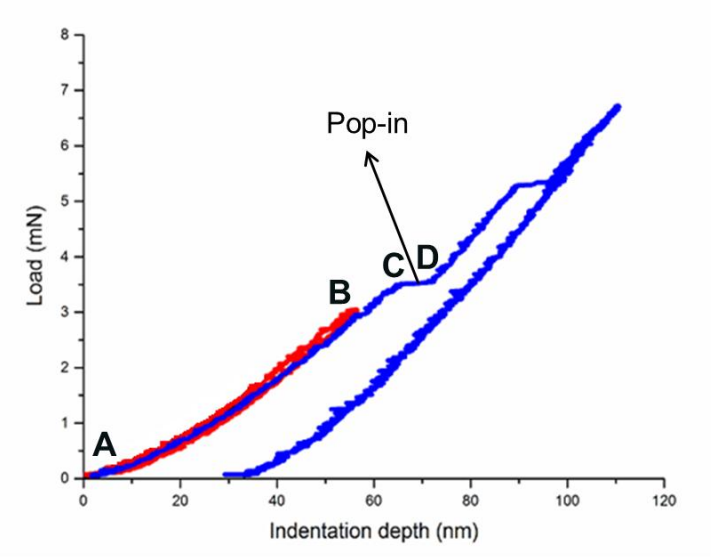

Fig. 2. Typical load-displacement response at loading rate of 0.1 mN/s showing cyclic loading to determine purely elastic deformation (AB) and first pop-in (CD)

DOI: 10.1016/j.jallcom.2013.12.002 To appear in: Journal of Alloys and Compounds, 2013

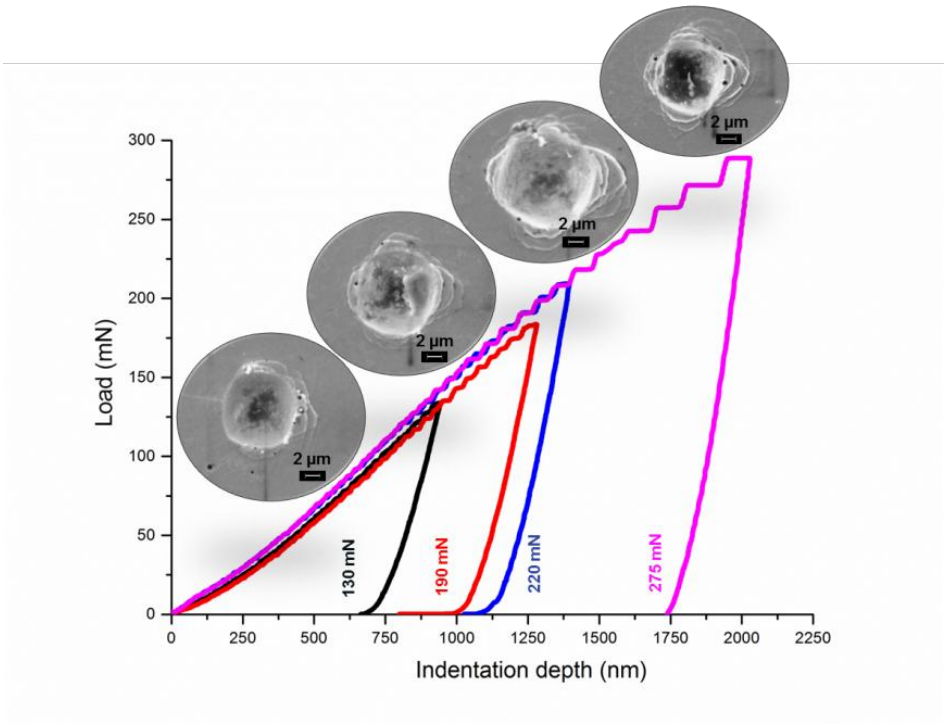

Fig. 3. Indentation load-displacement curves of ZrCu-based BMG for incremental loading-unloading at loading rate of 2 mN/s. The insets show evolution of shear-band patterns with increasing load.

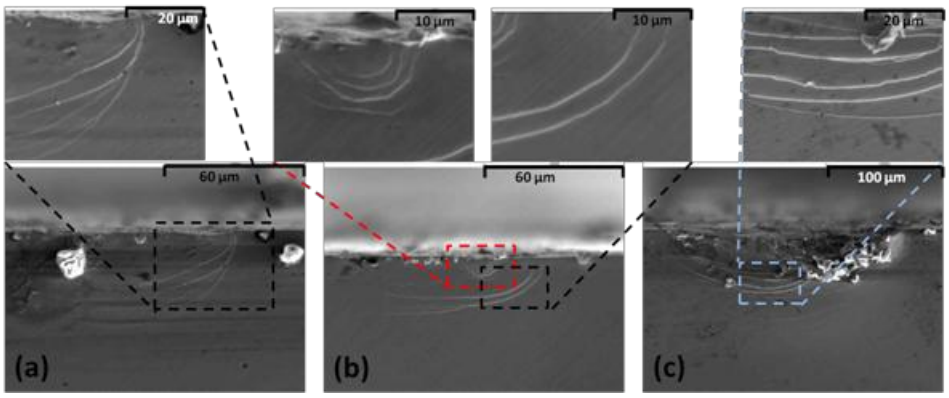

Fig. 4. Evolution of shear band localisation with increasing loads: (a) 2 kN; (b) 2.5 kN and (c) 4 kN

DOI: 10.1016/j.jallcom.2013.12.002 To appear in: Journal of Alloys and Compounds, 2013

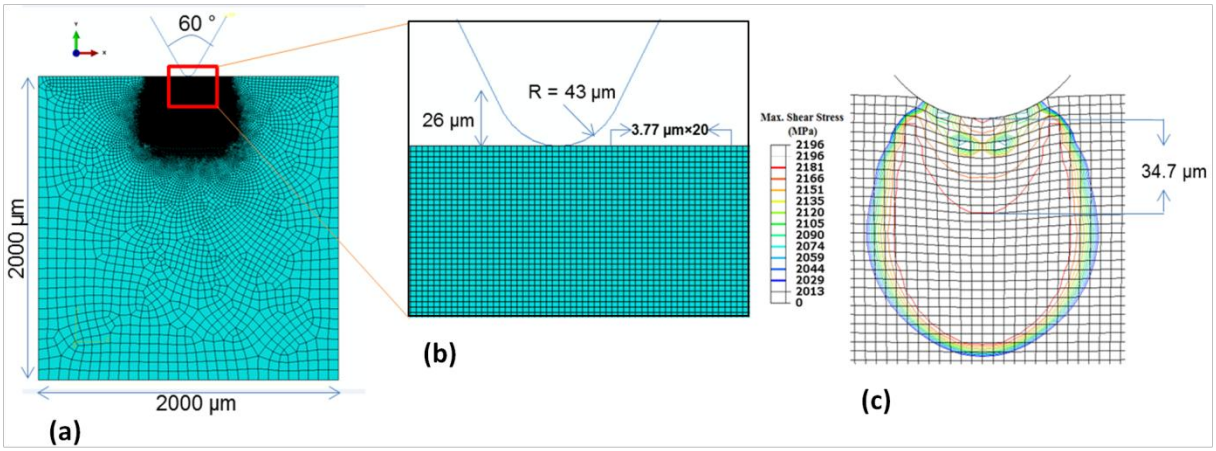

Fig. 5. (a) Finite element model of wedge indentation, (b) expanded view of the indenter geometry and the mesh density of the material, (c) maximum shear stress contour plot of the material after indentation with a 2 kN load.

Table. 1. Modelling parameters used in FEM simulation

Drucker-Prager parameters			Hardening	
β	Flow stress ratio	ψ		
0.01°	1	0.02°		
Shear damage parameters			Yield stress (MPa)	Plastic strain
Fracture strain	Shear stress ratio	Strain rate (s^{-1})	1900	0
0.05	1	0.016	1906.4	0.01574

DOI: 10.1016/j.jallcom.2013.12.002 To appear in: Journal of Alloys and Compounds, 2013